RSC Advances

ROYAL SOCIETY OF CHEMISTRY

www.rsc.org/advances

Journal Name

RSCPublishing

ARTICLE

CO_2 capture on easily regenerable hybrid adsorbents based on polyamines and mesocellular silica foam. Effect of pore volume of the support and polyamine molecular weight.

Cite this: DOI: 10.1039/x0xx00000x

Received 00th January 2012,
Accepted 00th January 2012

DOI: 10.1039/x0xx00000x

www.rsc.org/

Hang Zhang, Alain Goeppert,* Miklos Czaun, G. K. Surya Prakash,* George A. Olah*

Mesocellular foams (MCF) with a wide range of pore volume and pore size were prepared by varying a number of synthesis parameters such as ammonium fluoride concentration, effect of swelling agent trimethylbenzene (TMB), equilibration time and calcinations heating rate. The obtained MCF with pore volume from 0.98 cm^3/g to 4.17 cm^3/g were impregnated with polyethylenimine (PEI) having molecular weights of 800 g/mol to 25000 g/mol. These organic/inorganic hybrid materials with PEI loadings of 50 to 83% were tested for CO_2 adsorption capacity, kinetics, stability and regenerability. Increasing pore volume and size in MCFs allowed the loading of higher amounts of PEI and a better distribution of PEI in the pores. Access to the active amino sites by CO_2 was consequently facilitated. Adsorption of up to 6 mmol CO_2/g adsorbent (265 mg/g) were obtained at 85 °C with the adsorbent containing PEI with a molecular weight of 800 g/mol loaded on the support with the highest pore volume. Contrary to expectation, the adsorbents based on PEI with the highest molecular weight had faster desorption kinetics than the ones loaded with lower molecular weight PEIs. On the other hand the CO_2 adsorption kinetics for a given concentration were very similar with all the PEIs. The adsorption capacity of the adsorbents did not decrease over 100 adsorption/desorption cycles at 75 °C. The CO_2 adsorption results obtained here were in the top tier compared to the ones reported in the literature. Preparation of PEI based adsorbents clearly benefited from the utilization of supports with larger pore volume and diameter which in turn led to significantly improved CO_2 adsorption characteristics.

1. Introduction

Fossil fuels will remain the major energy source powering human activities for years to come. At current consumption rates, known petroleum oil natural gas, and coal reserves would last for about a century. Their availability could however be considerably extended by the exploitation of so-called non-conventional fossil fuels resources such as shale oil and gas as well as methane hydrates. New and emerging technologies for the location and economical extraction of these sources are being developed. Given their relative abundance and the fact that our current energy infrastructure is based predominantly on them, fossil fuels will continue to be exploited for as long as they can be economically produced.[1] One of the problem associated with the use of fossil fuels is that upon combustion they emit carbon dioxide, a major greenhouse gas (GHG). The emission of large amounts of CO_2 is now widely believed to be the cause for the currently observed climate change and associated environmental consequences such as ocean acidification and loss of biodiversity. Among the possible solutions to mitigate this problem, carbon capture and sequestration (CCS) has been proposed. Carbon capture and recycling (CCR) to synthetic fuels and materials is also a possible pathway.[1-3] Instead of being seen as a problematic greenhouse gas, the great potential of CO_2 as a raw material should be acknowledged.[4, 5] Carbon dioxide capture from relatively concentrated sources such as fossil fuel burning power plants and industrial sources is of particular interest. With improved adsorbents, the capture of CO_2 from the atmosphere could eventually also become economical.[6-8]

Among the existing CO_2 separation technologies,[9, 10] amine scrubbing which has been used industrially for many decades is one of the most suitable for high volume flue gas streams. In a typical process, 20 to 30% aqueous solutions of alkanolamines or proprietary hindered amines, such as monoethanolamine (MEA), diethanolamine (DEA) and KS-1 are used as adsorbents.[6, 11, 12] CO_2 is desorbed by heating the solution to a higher temperature, typically 100 – 140 °C. The large amount of energy required for the regeneration step is one of the major drawback of the aqueous amine systems. In addition, there are other significant problems, such as amine degradation, material corrosion and slow sorption/desorption kinetics.[7] Only a handful of small scale pilot plants have been

constructed and tested using this technology and others for the post-combustion CO_2 capture in coal fired power plants.

In order to reduce the energy requirement of the desorption step and avoid heating large amounts of water as well as overcome some of the other drawbacks of using liquid amines, solid adsorbents have been proposed as an alternative.[13-15] Physical adsorbents such as zeolites have been used in some industrial application for the separation of CO_2 and show high adsorption capacity for pure CO_2. However, they suffer from low selectivity due to the fact that CO_2 is only physically adsorbed on the surface. These physical adsorbents are therefore generally considered impractical for the separation of gases at low concentrations. In order to obtain a higher selectivity for CO_2 in a solid adsorbent, chemical adsorption applied to solids is a possibility. A number of approaches can be envisioned to achieve this goal such as (1) use of pure solid amines and polyamines as adsorbents,[16] (2) amines and polyamines chemically bound to the surface of a solid support,[17-22] (3) amines and polyamines physically impregnated on the surface of a solid support.[23-30] This latter option has been studied by a number of research teams. MEA and DEA have been deposited on various supports. However, due to their low molecular weight and relatively high volatility the solid adsorbents based on these amines had a tendency to leach the amine out, progressively reducing the adsorbents' capacity.[31, 32] Other low molecular weight amines such as pentaethyleneheamine (PEHA), tetraethylenepentamine (TEPA), diisopropylamine (DIPA) and 2-(2-Aminoethylamino)-ethanol had also similar leaching issues.[23] To avoid contamination of the gas stream and loss of activity over numerous adsorption/desorption cycles, it is important to select an amine with a sufficiently low vapor pressure. In this context, polyethylenimine (PEI), a polymeric amine bearing such characteristic has been impregnated on a number of supports and the obtained adsorbents studied for CO_2 adsorption.[13] Xu *et al*. reported the synergetic effect, with respect to adsorption capacity and sorption/desorption kinetics, between PEI and porous silica support, such as MCM-41, SBA-15 and developed the so-called "molecular basket" concept.[33-36] Our group has developed efficient, inexpensive and easy to prepare adsorbents based on PEI impregnated on fumed silica or precipitated silica. In the process of studying these sorbents, it was observed that the morphology of the porous material plays clearly a major role in the performance of the sorbents.[23, 24]

Several groups have studied the effect of pore structure and pore size of the support on the carbon dioxide adsorption capacity of the amine based sorbents. Zelenak *et al* prepared sorbents by grafting 3-aminopropyltriethoxysilane (APTS) to MCM-41, SBA-12 and SBA-15.[37] For the preparation of efficient amine-based mesoporous silicas they found the lower limit of the pore size to be about 35 Å. Below this size, the adsorption of CO_2 on the amine sites inside the pores was very limited due to limited diffusion into the pores. Son *et al* performed a study on a series of mesoporous material, MCM-41, MCM-48, SBA-15, SBA-16, and KIT-16 impregnated with PEI with a molecular weight (M_w) of 800 in a ratio of 1 to 1.[38] The adsorption capacity and adsorption kinetics increased primarily as a function of the pore size of the supports. They concluded that the average pore diameter was the most important variable dictating the adsorption capacity and kinetics. MCM-41 with the lowest pore diameter (2.8 nm) had the lowest CO_2 adsorption capacity. The use of KIT-6, with the largest pores (6.0 nm) in a 3D arrangement, resulted in the highest CO_2 adsorption capacity (135 mg CO_2/g adsorbent at 75 °C) which was believed to be due to an easier access to the active amino sites of PEI impregnated inside the pores. Yan *et al* prepared a series of SBA-15 based mesoporous materials with various average pore diameter and pore volume, and loaded them with 50% PEI (linear, M_w of 423).[39] They found that the absorption capacity was dependent on the total pore volume of the support rather than their pore diameter. In addition, the relationship between absorption capacity and pore volume was linear, supported by a strong correlation coefficient.

Although the reports of both Son and Yan allowed to gain some insight into the factors governing the preparation of efficient amine based mesoporous adsorbents, it seems that neither of their work was conclusive. First, their experimental protocols were very different. Son *et al* based their study on supports synthesized from different procedures. For example, MCM-41 used cetyltrimethylammonium bromide (CTMABr) as a templating agent, whereas SBA-15 and SBA-16 were prepared with triblock copolymers as surfactants. Although the resulting mesoporous materials were characterized by a set of values, namely surface area, average pore diameter and total pore volume, their properties and morphology could be different leading to accordingly different adsorbents. On the other side, Yan *et al* synthesized most of their supports based on the same procedure and only varied the aging time in the process.[39] However, the variety of the supports was probably too limited to draw a definitive conclusion. Yan *et al* listed only four supports, with a relatively narrow total pore volume distribution ranging from 0.7 cm^3/g to 1.2 cm^3/g, to determine that the adsorption capacity and pore volume are linearly related. Similarly, Son's supports only ranged from 2.8 nm to 6.0 nm in average pore diameter.

In regards of these limitations, a study with supports exhibiting a wider selection of average pore size and total pore volume but based on a similar synthesis method is clearly warranted. Recent development in the preparation of mesocellular foams (MCF) in which pore volume and size can be relatively easily tuned, make this type of support a good candidate for such a study.[40, 41] A series of MCFs were therefore prepared and tested as supports for PEI and their effect on CO_2 adsorption capacity and kinetics determined. Reaction conditions for the synthesis of the support have been screened to maximize its pore volume, pore diameter, and surface area. The resulting material features pore volumes of up to 4.17 cm^3/g, significantly surpassing similar materials reported in the literature. Combined with the high surface area, large pore diameter and interconnected wall structures, this material is suitable for loading PEI for the purpose of CO_2 separation. The obtained sorbents were tested for CO_2 adsorption capacity, kinetics, stability and regenerability.

2 Experimental

2.1 Chemicals

Triblock copolymer surfactant poly(ethylene oxide)-*block*-poly(propylene oxide)-*block*-poly(ethylene oxide) (P123, $EO_{20}PO_{70}EO_{20}$, M_w = 5800 g/mol, Aldrich), sodium silicate solution (26.5 % SiO_2, Aldrich), ammonium fluoride (Aldrich), glacial acetic

acid (EMD Chemicals), hydrochloric acid (EMD Chemicals), and *1,3,5*-trimethylbenzene (TMB, Alfa Aesar) were used to prepared the adsorbent supports. Deionized water (DI) was generated with a Milli-Q integral pure and ultrapure water purification system from Millipore. Two branched polyethylenemine (PEI) with molecular weights average (M_w) of ~25,000 g/mol and ~800 g/mol were purchased from Aldrich and denoted as PEI25k and PEI800, respectively. Branched PEI1800 (M_w ~ 1800g/mol) was purchased from Alfa Aesar. All chemicals were directly used as received unless otherwise stated.

2.2 Preparation of adsorbent supports

The mesoporous silica support was prepared by a "sol-gel approach". In a typical preparation of S5 (*vide infra*), 24.2 g P123 was added to 375 mL of DI water and 23 mL of glacial acetic acid. This mixture was kept under stirring at 40 °C for 18 h to obtain a homogenous solution. The pore swelling agent, 42 mL of *1,3,5*-trimethylbenzene (TMB) was added and the solution stirred for an additional 2 h. After that, 2.52 g of ammonium fluoride was added. Within a minute, a solution of 36 mL sodium silicate and 250 mL DI water was slowly poured into the prepared solution. The combined reaction mixture was vigorously stirred for 10 min before letting it sit under static conditions at 40 °C for 24 h. The temperature was increased to 70 °C and the solution aged for another 24 h. The resulting white suspension was filtered on a Buchner funnel and washed copiously with DI water. Any organic components present were removed by calcination at 560 °C for 6 h with a temperature ramp of 5 °C/min from room temperature to 560 °C to afford a light and fluffy white solid.

To study the effects of support composition and morphology on the CO_2 absorption capacity of the prepared adsorbents, a series of mesoporous silica support were synthesized by modifying various variables as well as based on previous reports. More details are given in the SI.

2.3 Preparation of adsorbents

PEI was coated on the supports by a wet impregnation method. Desired amounts of PEI and support were mixed in methanol solution. After mixing for 24 h, the methanol was evaporated on a rotary evaporator. The prepared adsorbent was further evacuated under high vacuum at r.t. overnight. Samples were labeled as MCF-x, where x represents the PEI weight percentage. All adsorbents were stored in closed vials until further investigation

2.4 Measurement of CO_2 adsorption capacity

The CO_2 adsorption and desorption measurements were performed on Shimadzu TGA-50 thermogravimetric analyzer. Usually the adsorbents were tested for CO_2 adsorption at 25, 55, and 85 °C using a 95% CO_2/5% N_2 gas mixture.

Typically 5 mg of solid adsorbent was loaded in a platinum pan and placed into the TGA instrument. The sample was initially heated to 110 °C under a pure N_2 atmosphere (flow = 60 mL/min) and this temperature was maintained for 30 minutes to desorb water and CO_2 from the surface. The temperature was then lowered to 25°C and the adsorbent exposed to 95% CO_2 (flow = 60 mL/min) for 3 h. After that the gas flow was switched back to N_2 and the temperature increased to 85 °C for 90 minutes desorption. The second adsorption cycle was carried out under 95% CO_2 at 55 °C for 3 h followed by desorption at 85 °C under N_2 for 90 minutes. The third adsorption cycle was carried out at 85 °C for 3h. Finally 10 adsorption/desorption cycles were carried out isothermally at 85 °C. Fifteen minutes adsorption under 95% CO_2 was followed by 25 minutes desorption under N_2 for each cycle.

For regenerability studies, under isothermal conditions with 100 adsorption/desorption cycles or more, the adsorbent sample was pre-treated as described above (110 °C). The temperature was then lowered to 75 °C. For each cycle, an adsorption step at 75 °C (10min) under 95% CO_2 (60 mL/min) was followed by a desorption step at 75 °C (15 min) under pure N_2 (60 mL/min).

2.5 Characterization

2.5.1 Surface area and pore analysis. Nitrogen adsorption/desorption isotherms were measured at -196 °C with a Quantachrome NOVA 2200e surface area and pore volume analyzer. The samples were pre-treated at 250 °C under vacuum for at least 3 h. The specific surface area was calculated by the multipoint Brunauer-Emmett-Teller (BET) method. The total pore volume was evaluated at a P/P_0 close to 0.995. The Barrett-Joyner-Halenda (BJH) method was used to calculate the pore volume and pore size distribution using the desorption branch of the isotherm. A transmission electron microscope (TEM, JEOL JEM-2100F) was used to observe the morphologies of the supports and adsorbents.

2.5.2 Thermogravimetric analysis to determine the organic content of the prepared adsorbents. The organic content of the adsorbents was determined by weight loss using thermogravimetric measurements on a Shimadzu TGA-50 thermogravimetric analyzer under an air flow of 30 mL/min in a temperature range increasing from 25 to 800 °C with a heating rate of 10 °C/min.

2.5.3 Density measurements. The tapped density of the adsorbent was measured by placing a known amount of the adsorbent into a graduated cylinder, which was tapped continuously for 2 minutes. The volume occupied by the adsorbent was then recorded and the density of the solid in g/mL determined.

3. Results and discussion

3.1 Preparation of MCF supports: screening of synthesis conditions

Part of the procedural work was based on Genggeng Qi *et al*[42] and Schimidt *et al*'s papers.[40] Reaction conditions have been screened to improve the structure and morphology of the support to suit our needs. Specifically, the effects of ammonium fluoride concentration, rate of heating during the calcination process and equilibration time of TMB were studied.

3.1.1 Effect of ammonium fluoride concentration during MCF preparation. Ammonium fluoride plays several roles in the synthesis of mesoporous materials. First, it is a mineralizer that increases the solubility of silicate. Second, it catalyzes the oxolation

reaction and enables the building of the oxide framework.[43] In addition, the NH_4F/Si molar ratio promotes the enlarging of the window size and may possibly produce mesostructures that suits our needs.[40]

The effect of the ammonium fluoride concentration is shown in Table 1 and Figure 1(a-c). By altering the [NH_4F]/[Si] molar ratio in the system during the preparation, the morphology of the supports is varied (see SI for detail about the preparation). The highest surface area was obtained when no NH_4F was used. However, the average pore size and pore volume were the lowest in the absence of NH_4F. The initial addition of NH_4F significantly decreased the surface area, but the trend plateaued for [NH_4F]/[Si] ratios higher than 0.86 staying at around 600 m^2/g. Both average pore diameter and pore volume increased until the [NH_4F]/[Si] ratio reached a value of about 0.5, after which they increased only moderately or plateaued. From Table 1 it can be seen that under these conditions, ammonium fluoride helps to expand the pore diameter and pore volume but has a somewhat negative effect on the surface area.

Using tetraethyl orthosilicate (TEOS) as a silica source, Schmidt-Winkel *et al*[40] achieved excellent mesostructures when the [NH_4F]/[Si] molar ratio was 0.03, which was significantly lower than the ratio we used with sodium silicate as the silica source. In the present study, we selected sodium silicate because the formed foam would have more hydroxyl groups on its surface, helping to bind more strongly the impregnated PEI, while at the same time also potentially increasing the hydrothermal stability of the adsorbent.

Table 1. Physical data for supports prepared with various NH_4F concentrations

Experiment #	[NH_4F]/[Si]	Surface area (m^2/g)	APS (A)	PV (cm^3/g)
S-[NH_4F]-0	0.00	942	46	1.09
S-[NH_4F]-0.09	0.09	788	75.8	1.49
S-[NH_4F]-0.42	0.42	694	101	1.77
S-[NH_4F]-0.86	0.86	622	104	1.61
S-[NH_4F]-1.28	1.28	724	119	2.15
S-[NH_4F]-1.71	1.71	607	110	1.68
S-[NH_4F]-2.57	2.57	600	127	1.90

3.1.2 Effect of the heating rate during the calcination process. Calcination is the final step in the preparation of mesocellular silica foam. It thermally condenses the silica framework as well as removes the organic template and water. Typical calcination temperatures to remove the surfactant P123 and organic components are generally between 500 and 700 °C. Early in the development of mesoporous materials, a slow heating rate was recommended to avoid a possible collapse of the porous network. Therefore, 1 or 2 °C/min has been the standard heating rate for preparing mesoporous materials of the M41S family, HMS, MSU-X, SBA-15, etc. This protocol was challenged after Bagshaw *et al* experimented with fast heating rate of up to 100 °C/min. They observed that due to the low combustion temperature of PEO based templates, low heating rates resulted in the sample being without pore filling for a longer time affecting the structure of the mesoporous solid. In the case of Si-MSU-X in particular they noticed that its structural integrity is best preserved when exposed to the calcinations for the shortest period of time, i.e. at the fastest rate of heating.[44]

Here, we investigated the effect of heating rate on the mesostructure of the supports. As shown in Table 2, among the heating rates we tested (1 °C/min, 2 °C/min, 5 °C/min, and 10 °C/min), an intermediate rate of 5 °C/min maximized at the same time the surface area, average pore diameter and pore volume. Although different systems may be optimized at different heating rates, in the case of the present support, the heating rate of 5 °C/min was found to be optimal to obtain the largest pore volume with correspondingly large surface area and average pore diameter.

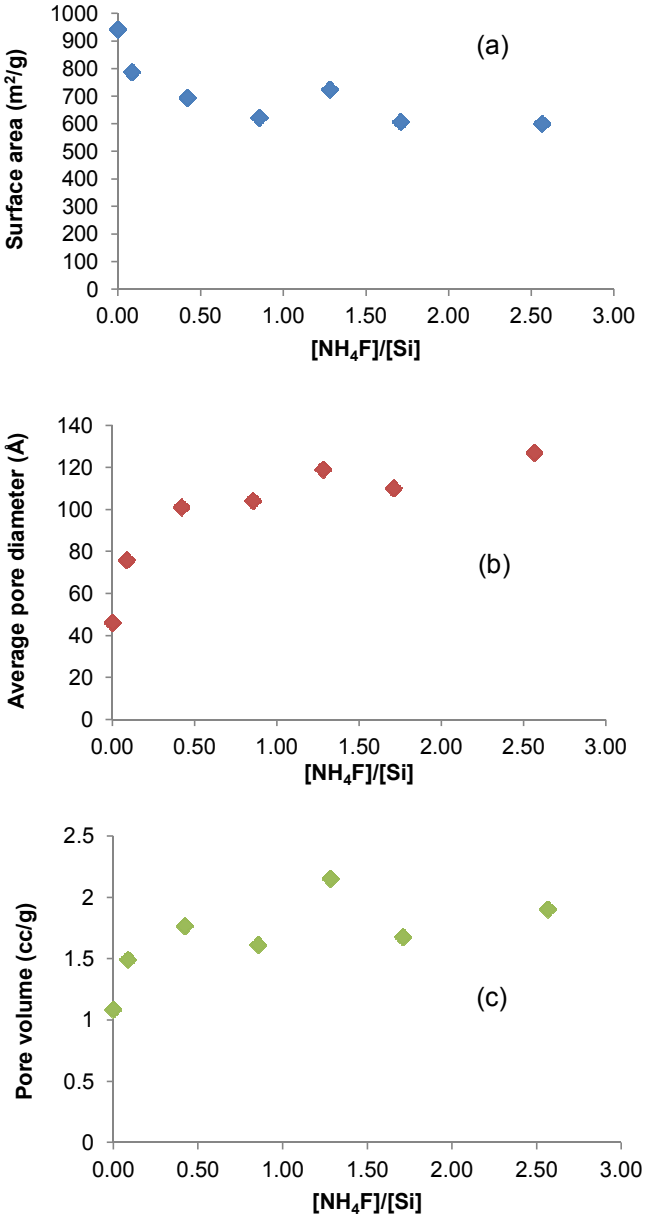

Fig. 1 Influence of the concentration of ammonium fluoride on (a) the surface area of MCF (BET), (b) the average pore diameter of MCF, (c) the total pore volume of MCF.

Table 2. Effect of heating rate on the physical characteristics of MCFs

Experiment #	Heating rate (°C/min)	Surface area (m^2/g)	APD (Å)	PV (cm^3/g)
S-1C/min	1	492	150	1.85
S-2C/min	2	519	129	1.67
S-5C/min	5	543	154	2.10
S-10C/min	10	606	122	1.85

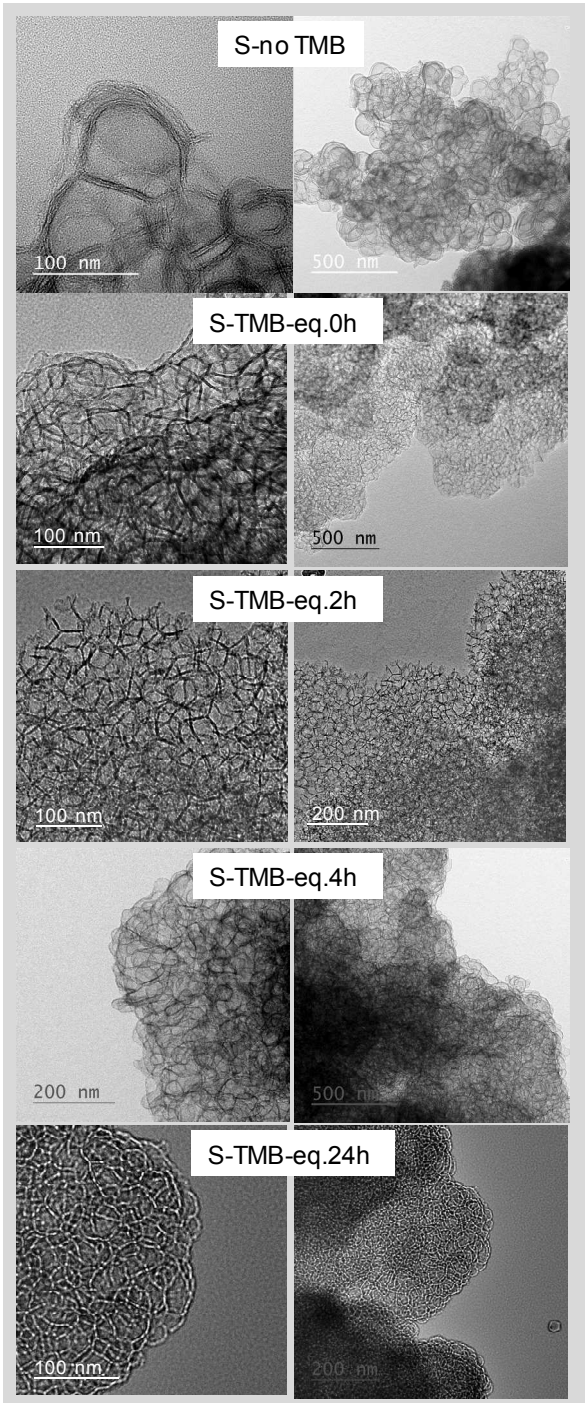

Fig. 2 TEM pictures of supports prepared with and without TMB and after various equilibration times.

Effect of the addition of swelling agent TMB. For the purpose of loading PEI to absorb CO_2, mesoporous cellular foam with interconnected voids is preferred to allow easy diffusion of CO_2 through the material. With this in mind, the swelling agents trimethylbenzene (TMB), was added to the system, not only serving the role of expanding pore volume and pore size, but also potentially to create more channels by breaking down the ordered mesoporous structure.[41, 45]

We monitored the addition of TMB and the effect of equilibration time on the pore structure. As shown in Table 3, when no TMB is added, surface area, average pore diameter and pore volume are the lowest in the series at 543 m^2/g, 154 Å and 2.1 cm^3/g, respectively. Initial addition of TMB, even without any equilibration time improved all these parameters. An equilibration time of 2 hours allowed a further significant increase for all these parameters. Surface area increased to 688 m^2/g whereas the pore volume doubled compared to the support prepared without TMB (4.17 cm^3/g versus 2.1 cm^3/g). Longer equilibration time (24 hours) did not result in further expansion of the pore diameter and volume. On the contrary, average pore diameter decreased to 203 Å, and total pore volume decreases to 3.34 cm^3/g.

Meanwhile, all the samples were analyzed under TEM (Figure 2). As shown in Figure 2, shorter equilibration time in the presence of TMB led to a structure resembling "tree branches", while 24 hours of equilibration time resulted in a closed spherical structure. Further evidence (*vide infra*) suggests that adsorption is more effective when PEI was loaded on the "tree branched" support. Indeed the tree branched material seems to have better diffusive characteristics.

From the perspective of accommodating more PEI for CO_2 adsorption, pore volume is of primary importance, because it is the pore volume which determines how much PEI can be loaded inside the pores. PEI has a density of 1.03 g/cm^3. One gram of MCF with for example a PV of 1.5 cm^3/g can thus theoretically load a maximum of 1.6 g of PEI inside its pores. According to the theory of synergistic enhancement, the CO_2 adsorption performance is closely related to the portion of PEI loaded inside the pore.[25] Therefore, pore volume is the major factor. In addition, pore diameter and window opening are also important factors, considering the process of CO_2 adsorption by PEI. Large pore diameters and windows openings facilitate the accessibility of the PEI's active amino groups by CO_2.

Table 3. Effect of the addition of trimethylbenzene (TMB) and equilibration time on the structure of MCFs

Experiment #	TMB/P123 (w/w)[a]	Equilibration time (h)	Surface area (m^2/g)	APS (Å)	PV (cm^3/g)
S-noTMB	0	--	543	154	2.1
S-TMB-eq.0h	1.75	0	618	191	2.96
S-TMB-eq.2h	1.75	2	688	243	4.17
S-TMB-eq.4h	1.75	4	796	152	3.03
S-TMB-eq.24h	1.75	24	658	203	3.34

[a] Weight ratio using 42g TMB.[40]

3.2 Preparation of CO_2 adsorbents based on MCF and PEI

3.2.1 Characteristics of the supports tested for the preparation of CO_2 adsorbent with PEI. The CO_2 adsorbents where prepared from PEI and MCF by simple mixing of the components in methanol followed by evaporation of the solvent under vacuum (see experimental section). In a first series of experiments, the effect of the morphology and structural characteristics (surface area, pore volume, pore diameter) of various MCF supports on the CO_2 adsorption capacity was studied. Five supports described in Table 4 with a wide range of pore volume and diameter were chosen and classified following their total pore volume from S1 to S5 (see the SI for details on the preparation of these supports). The supports all followed a type IV adsorption isotherm characteristic of mesopores (20 to 500 Å) within the solid (Figure 3). This can be clearly seen in the pore size distribution measured following the BHJ method (Figure 4). The surface areas of these supports were in a range from 519 – 688 m^2/g, sufficient for loading PEI through silanol group hydrogen bonding and physical interaction with the support. This variation in the surface area remained, however, relatively modest compared to the variation in average pore diameter and total pore volume. The average pore diameter increased from 65.7 Å to 243 Å going from S1 to S5; an increase of 270%. Total pore volume varied from 0.98 cm^3/g to 4.17 cm^3/g from S1 to S5; an increase of 325%. The use of these series of supports should advance the understanding of the effect of pore volume and pore diameter on the PEI impregnation and CO_2 adsorption. S1 to S3 were prepared in the absence of the swelling agent TMB and had a very similar maximum at around 85Å in the pore diameter distribution (Figure 4). There was, however, a clear shift of the tail of the curve towards higher pore diameters when going from S1 to S3 explaining to some extent the increase in cumulative pore volume from S1 to S3 (Figure 5). S4 and S5 prepared in the presence of TMB had a wider pore diameter distribution which was also shifted toward larger pore diameter. S5, the MCF with the largest total pore volume had also the largest average pore diameter. From Figure 5 it can also be observed that in the case of S5 most of the porosity is due to pores with a diameter larger than ~120Å, which is fairly large. All the supports had, however, a quite broad distribution in pore diameter.

Table 4. Characteristics of the supports used in the study of the effect of pore volume and pore diameter on the preparation of PEI-based adsorbents and their CO_2 adsorption capacity

Support	Surface area (m^2/g)	Average pore diameter (Å)	Total pore volume (cm^3/g)	Pore diameter distribution	Reference [(a)]
S1	596	65.7	0.98	small peak at 35 Å, big one at 85 Å	---
S2	519	129	1.67	broad peak from ~60 Å to ~200 Å	S-2C/min
S3	543	154	2.10	broad peak from ~60 Å to ~200 Å	S-no TMB S-5C/min
S4	618	191	2.96	Very broad peak from ~40 Å to ~200 Å	S-TMB-eq.0h
S5	688	243	4.17	Very broad peak from ~60 Å to ~250 Å	S-TMB-eq.2h

[(a)] See SI for detailed description of the synthesis of these supports

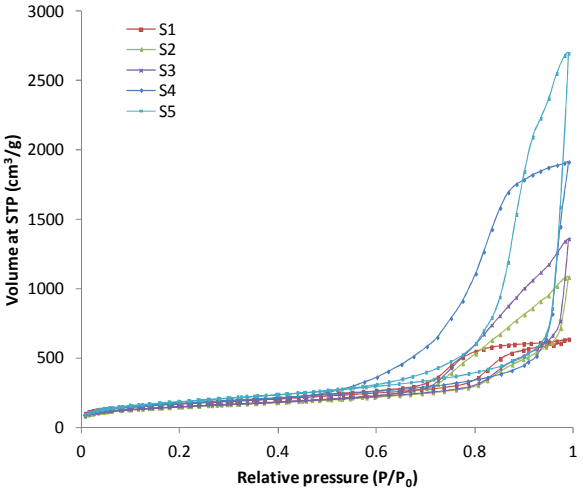

Fig. 3 N_2 adsorption/desorption isotherm for MCF S1 to S5.

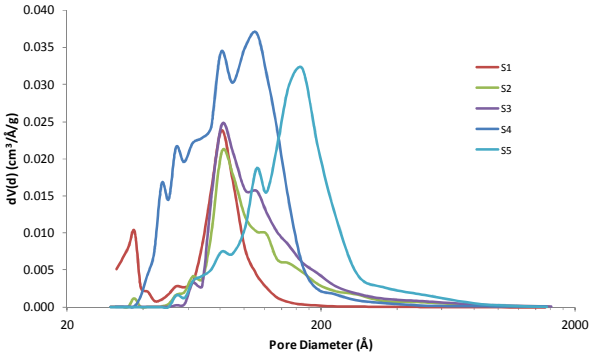

Fig. 4 Pore size distribution of MCF S1 to S5.

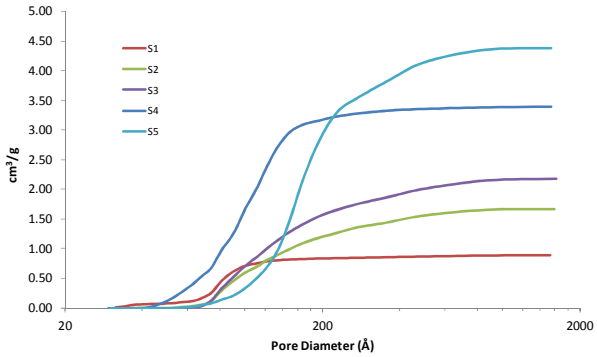

Fig. 5 Cumulative pore volume as a function of pore diameter of MCF S1 to S5

3.2.2 Preparation and characteristics of the adsorbents prepared with PEI. Polyamines impregnated MCF have been studied by a few research groups in recent years.[42, 46, 47] Zhao *et al*. reported the use of PEI-MCF for the adsorption of CO_2.[48] However this study included only one MCF with a pore volume of 3.14 $cm^3.g^{-1}$ and a pore diameter of 113 Å. Chaffee *et al.* also tested PEI/MCF[49] to

selectively adsorb CO_2 whereas Jones *et al.* used poly(allylamine)/MCF[50]. Here again only one or two MCF supports with a limited range in pore volume and surface area were employed. Amine and polyamines chemically bound on the surface MCF have also been considered by Jones et al,[51] Chaffee et al.[52] and others.[46]

In the present paper branched PEI with a high molecular weight of 25,000 g/mol (PEI25k) was selected for the experiments in large part because of its low volatility.[23, 24] On the five selected supports (S1 to S5), PEI25k was loaded through a typical impregnation method (see experimental section). Weight ratios of support vs. PEI25k were 1:1, 1:2, 1:3, 1:4, and 1:5, corresponding to a PEI loading of 50%, 67%, 75%, 80% and 83%, respectively. All the selected supports formed free flowing white powders when impregnated with PEI at contents of 50% and 67% (Table 5). However, when the PEI content was further increased to 75%, using the support with the lowest pore volume resulted in the formation of a sticky solid that was not suitable for CO_2 adsorption applications. The maximum amount of PEI which could be loaded on this support had been exceeded. Proceeding to higher PEI loadings a similar phenomenon was observed for supports with higher pore volumes and pore diameters. S2 and S3 with a pore volume of 1.67 and 2.10 cm^3/g, respectively, did not form a free flowing solid at a loading of 80% PEI. With a PEI content of 83% only S5, the support with the highest pore volume (4.17 cm^3/g), was able to form a suitable solid adsorbent. The fact that larger amounts of PEI could be loaded on the supports with a higher pore volume seems logical.

Table 5. Aspect of the adsorbents prepared from MCF and PEI25k

Support	50% PEI	67% PEI	75% PEI	80% PEI	83% PEI
S1	solid	solid	Sticky solid	NP	NP
S2	solid	solid	solid	Sticky solid	NP
S3	solid	solid	solid	solid	NP
S4	solid	solid	solid	solid	Sticky solid
S5	solid	solid	solid	solid	solid

NP: not prepared

Table 6. Surface area (BET, m^2/g) of the adsorbents prepared from MCF and PEI25k

Support	No PEI	50% PEI	67% PEI	75% PEI	80% PEI	83% PEI
S1	596	TS	TS	Sticky solid	NP	NP
S2	519	59.8	11.1	TS	Sticky solid	NP
S3	543	57.8	13.3	3.84	TS	NP
S4	618	82	40	10.5	0.73	Sticky solid
S5	688	132	51.5	15.5	4.1	TS

TS: too small for measurement; NP: not prepared

Table 7. Total pore volume (cm^3/g) of the adsorbents prepared from MCF and PEI25k

Support	No PEI	50% PEI	67% PEI	75% PEI	80% PEI	83% PEI
S1	0.98	TS	TS	Sticky solid	NP	NP
S2	1.67	0.43	0.050	TS	Sticky solid	NP
S3	2.10	0.50	0.085	0.025	TS	NP
S4	2.96	0.70	0.32	0.082	0.0022	Sticky solid
S5	4.17	1.12	0.45	0.10	0.0175	TS

TS: too small for measurement; NP: not prepared

The surface area and total pore volume of all the usable adsorbents (i.e. non-sticky solids) were also measured and the results are presented in Tables 6 and 7, respectively. As a general trend, the surface area decreased with increasing PEI loading (see also SI, Figure S1). The total pore volume pattern followed the same pattern as can be seen in Table 7 as well as Figure 6. However, for a similar PEI loading the supports with the highest initial total pore volume were able to retain a higher surface area than supports with a similar surface area but lower total pore volume. A higher pore volume of the support (Table 4) is therefore highly important for the preparation of adsorbents able to accommodate high PEI loading while retaining reasonable surface area and pore volume to allow an easier access for CO_2 molecules. Figure 7 shows the pore size distribution of the support with the highest pore volume (S5) impregnated with various amounts of PEI25k. It can be noticed that despite an obvious decline in pore volume, the pore size distribution does not change dramatically going from a concentration of 50 to 75% with a peak at around 140 Å and 160 Å, respectively. At a PEI concentration of 80%, no more peak is discernible in the pore size distribution as most of the porosity disappears. This indicates that even at loadings as high as 75%, some large pores are still present which probably allow an easier access to the active amino sites for CO_2. The adsorbents with favorable physical properties, i.e. free flowing solids, were tested for CO_2 adsorption.

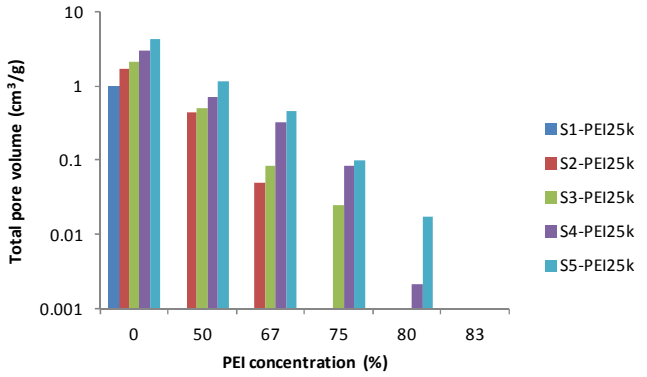

Fig. 6 Total pore volume of adsorbents based on MCFs as a function of PEI25k loading in the adsorbent.

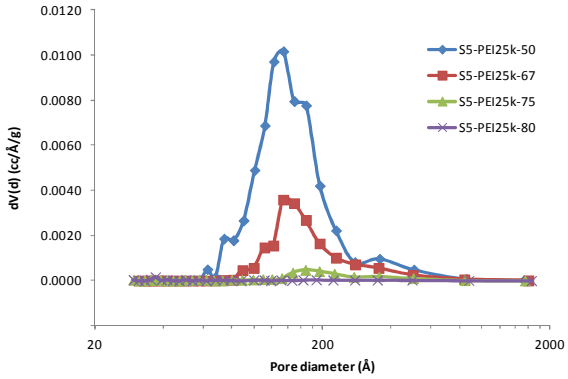

Fig. 7 Pore distribution of S5 MCF impregnated with PEI in various concentration.

3.3 CO_2 Adsorption capacity measurements

The CO_2 adsorption capacity of each sorbent was measured by TGA. The sorbent was first heated to 110 °C under nitrogen (60 mL/min) to desorb CO_2 and water present on the surface. The flow was then switched to 60 mL/min pure CO_2 for 180 min for adsorption followed by 60 mL/min pure nitrogen at 85 °C for 90 min in the desorption step. This procedure was repeated for 25 °C, 55 °C, and 85 °C to determine the influence of temperature on the CO_2 adsorption. The results are presented in Table 8 as well as in Figures 8 and 9.

It can be observed that, as a general trend, the adsorption capacity at a given temperature and concentration of PEI25k increased with increasing pore volume and pore diameter of the support. For example at 25 °C and a concentration of PEI25k of 50%, the CO_2 adsorption capacity increased from 0.53 mmol CO_2/g for S1 to 1.78 mmol/g for S5. A similar effect was observed at higher PEI25k loadings and temperatures. This agrees with previous studies conducted by other groups, suggesting that adsorption capacity benefits from larger pore size and/or larger pore volume (see introduction).[37-39]

At 25 °C, the highest adsorption was obtained at the lowest loading of 50% PEI on all the supports (Figure 8a and 9a). At a temperature of 55 °C, the adsorption capacity displayed a maximum at 67% PEI for all supports except S1 with the lowest pore volume which had the highest adsorption at a PEI loading of 50% (figure 8b and 9b). At 85 °C, the increase in PEI concentration resulted generally in an increase in the CO_2 adsorption capacity. This increase was however most pronounced at lower loadings, i.e. between 50 and 67% (Figure 8c). At higher loadings, the adsorption reached a plateau and the addition of larger amounts of PEI did not improve further the adsorption capacity. In the case of S3, the adsorption even decreased when the PEI loading was increased from 75 to 80% probably due to the filling of the pores by PEI.

Raising the temperatures had a positive effect on the adsorption capacity of pure CO_2 which increased accordingly on all supports and PEI loadings above 50%. This pattern is the opposite of the one usually observed with commonly used liquid amines for CO_2 capture such as MEA and DEA. A similar trend had already been observed by us and others when using PEI as the active component in supported amines.[23, 33] It is probably due to the nature of PEI25k which is a very viscous gel. Lower viscosity at higher temperature is believed to result in a better accessibility of the amino groups of the adsorbent for CO_2 molecules and improved reaction kinetics, leading to higher CO_2 adsorption.[33] This effect is more pronounced in adsorbents with higher concentrations of PEI, where PEI is less uniformly dispersed on the solid support. With increasing PEI loadings, the surface of the support is increasingly saturated with PEI and access to some amino groups is made more difficult.

An optimal utilization of the amino groups in PEI is also of importance. As shown in Figure 10, at 25 °C, PEI was used most efficiently at the lowest loading of 20% PEI on S5 with 250 mg CO_2 adsorbed per g of PEI in the adsorbent. At this temperature, the role of temperature in assisting CO_2 diffusion is relatively weak. The accessibility of amino groups depends largely on the total pore volume of the adsorbent left over after loading PEI. Therefore, we observed an almost linear relationship between the PEI efficiency and loading at 25 °C. As mentioned above, the adsorption reaction is exothermic, and increasing temperature should theoretically lower the adsorption capacity. It was the case for S5-PEI25k-20 which went from an adsorption capacity of 250 mg CO_2/g PEI at 25 °C to 130 mg CO_2/g PEI at 85 °C. However, for adsorbents with higher PEI content, the adsorption capacities being dependent on both thermodynamic and kinetic parameters, this order differed. Adsorption is thermodynamically disfavored by higher temperature, but is kinetically favored, because higher temperature facilitates CO_2 diffusion and access to the active sites. At 50 °C, an optimal utilization of PEI was realized at a loading of about 50% PEI. At 85 °C, utilization of PEI was the best at a PEI loading around 70% PEI with ~300 mg CO_2/g PEI. This was also the highest value of all temperatures studied.

This behavior on MCF supports is somewhat different from the one observed on PEI/fumed silica in which the highest adsorption capacity per g of PEI at 85 °C was obtained at PEI loadings below 50% (~350 mg CO_2/g PEI) with a decrease in capacity when going to higher PEI concentrations.[23]

Although a higher PEI loading might increase the overall CO_2 adsorption capacity of the adsorbent based on MCF, depending on the temperature, the most effective use of the polyamine might be achieved at lower loadings. Besides the total adsorption capacity, other important parameters include kinetics of adsorption and desorption. A better dispersion of PEI can induce a faster desorption of CO_2 during the regeneration step. Observed desorption was therefore faster in adsorbents with lower PEI loadings as can be seen in Figure 11 showing the percentage of desorption as a function of time on S5-PEI25k. The desorption time gradually increased going from a PEI25k content of 50% to 83% on S5-PEI25k. Whereas on S5-PEI25k-50 the desorption was nearly complete after only 3 min, almost 15 min were necessary to achieve the same with S5-PEI25k-83.

On the other hand, the bulk density of S5-PEI25k increased significantly from 0.11 g/mL for the adsorbent containing 50% PEI to 0.40 g/mL for the one containing 83% PEI (see SI, figure S2). PEI filling progressively the pore volume of the support, S5, the bulk density should follow a relatively linear path with increasing PEI concentration. This is indeed the case from loadings of 50% PEI up to about 80%. After that, the density increased sharply. This could be due to the pore volume inside the MCF being nearly all occupied by PEI at loadings of ~80% PEI (Figure S2 b). PEI having a density of 1.03 ml/g, at 80% loading, 1 g of adsorbent contains 0.8g, or 0.777 mL of PEI. The other 0.2g is the support. At 4.17 mL/g of pore volume, 0.2g of S5 support contains about 0.834 mL of pores. This is very close to the 0.777 mL of PEI on this S5-PEI25k-80. It is also likely that not all the pores can be filled by high molecular weight PEI and we may have reached the limit of the pore volume available inside S5. At a higher loading of 83% PEI, 0.806 mL are needed to accommodate all the PEI. However, only 0.709 mL volume is available in the support (0.17 x 4.17 mL/g). Thus, there is an excess of PEI compared to the volume available in the support. This excess PEI is most likely impregnated outside of the support particles, leading to agglomeration of these particles and the observed sharp increase in density.

At 85 °C, an adsorption capacity of 0.33 and 2.1 mmol CO_2/mL adsorbent for S5-PEI25k-50 and S5-PEI25k-83, respectively (Figure S3 and table S1) were measured. This six-fold increase in CO_2 adsorption capacity per mL is much higher than what would be expected from a simple increase in PEI concentration from 50 to 83 %. This increase in adsorption capacity was progressively less pronounced at lower temperatures of 55 °C and 25 °C. On a volume basis, the use of adsorbents with a higher PEI content remains, however, advantageous as it would reduce the overall size and capital cost of the adsorption unit.

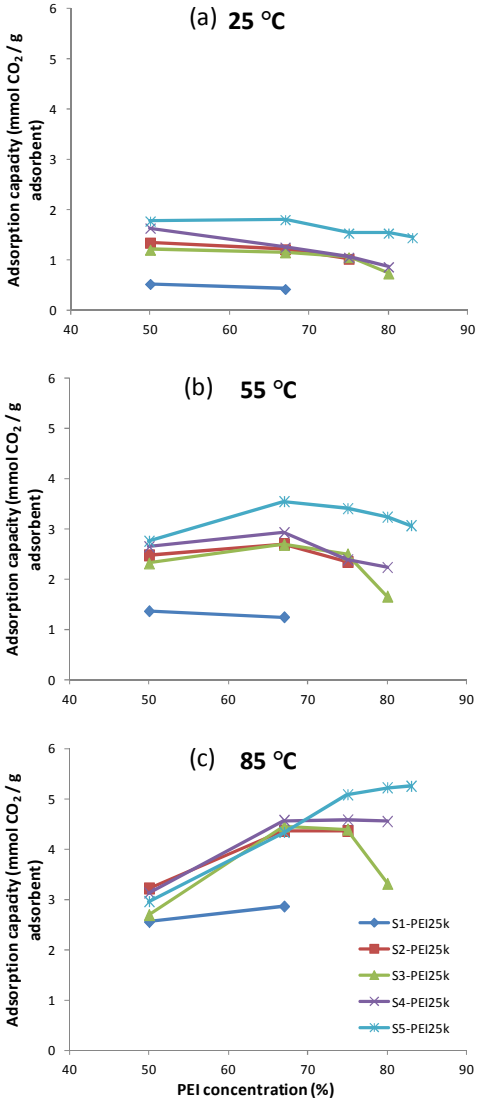

Fig. 8 CO_2 adsorption capacity on Sx-PEI25k as a function of PEI loading. (a) 25 °C, (b) 55 °C, (c) 85 °C.

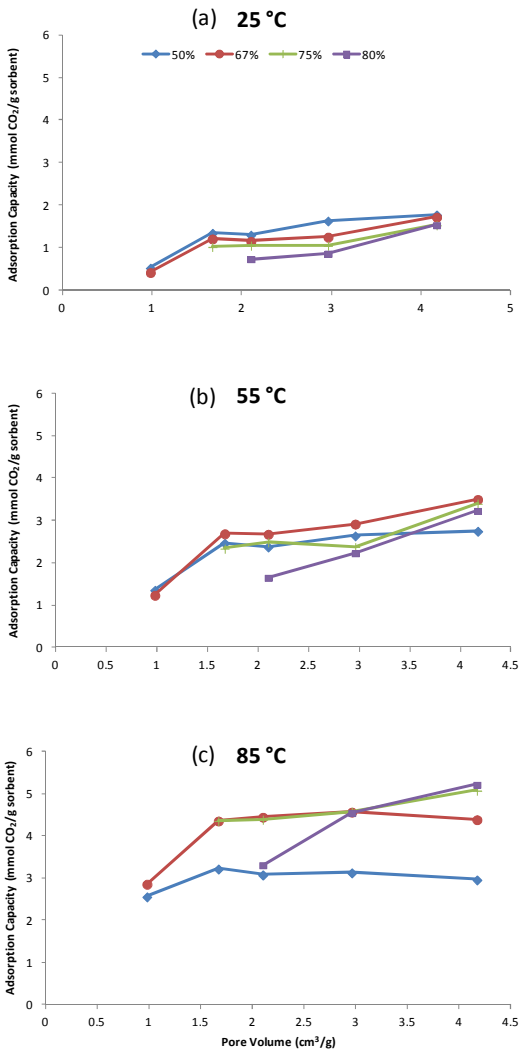

Fig. 9 Effect of the pore volume of the support on CO_2 adsorption capacity of adsorbents prepared with various concentrations of PEI25k. (a) 25 °C, (b) 55 °C, (c) 85 °C.

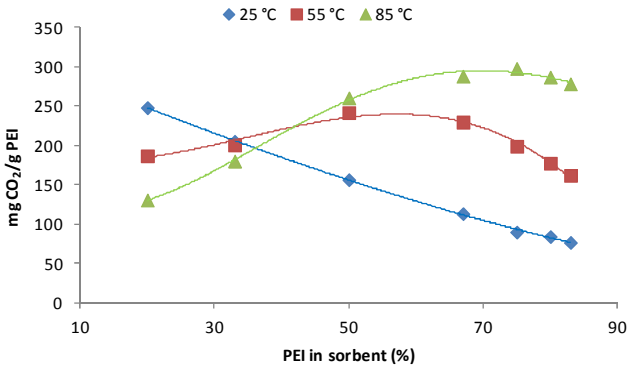

Fig. 10 Effectiveness of PEI utilization. CO_2 Adsorption capacity in mg CO_2/g PEI in the adsorbent measured at various temperatures on S5-PEI25k as a function of PEI loading.

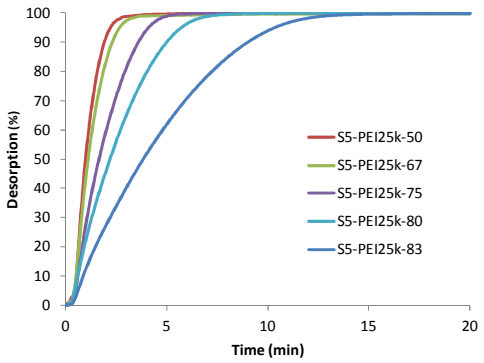

Fig. 11 Desorption completion at 85 °C as a function of time of adsorbents based on S5 containing PEI25k loadings from 50% to 83%.

3.3.1 Effect of the molecular weight of PEI on CO_2 adsorption. It has previously been shown that the lower the molecular weight of PEI, the higher the CO_2 adsorption capacity of the adsorbent.[23] When impregnated on fumed silica in a ratio of 1:1, linear PEI with a M_w of 423 adsorbed 173 mg CO_2/g adsorbent. Similar adsorbents prepared with branched PEI with a M_w of 800 and 25000 adsorbed 147 mg CO_2/g and 130 mg CO_2/g, respectively. Shorter oligomers such as pentaethylenehexamine (PEH) and tetraethylenepentamine (TEP) adsorbed the most at 192 mg CO_2/g and 200 mg CO_2/g, respectively. The higher adsorption capacity of ethylenimine oligomers and linear PEI can most probably be attributed to the fact that these contain only primary and secondary amines which are both active for CO_2 capture. The higher molecular weight PEI used were branched and therefore contained beside primary and secondary amines also tertiary amines which under dry conditions do not adsorb CO_2. In addition to this, the viscosity of branched PEI is higher, which also hinders the access to the active amino sites on the adsorbent.

The problem with ethylenimine oligomers and to some extent the low molecular weight PEIs is their stability over time. Because of their lower boiling point and therefore increased volatility, they had a tendency to leach out part of the amine, resulting in a loss of adsorption capacity over numerous adsorption/desorption cycles as well as possible contamination of the system downstream of the adsorbent narrowing the adsorbents' practical application. In order to avoid these potential problems as much as possible we decided to limit our present study of the effect of molecular weight on the adsorption capacity of MCF-PEI to branched PEIs with M_w of 800, 1800 and 25000. These PEIs were impregnated on the support with the highest pore volume (S5) to allow loadings of up to 83% PEI. To determine the effect of temperature the CO_2 adsorption capacity was measure at 25 °C, 55 °C and 85 °C. The results can be seen in Figure 12.

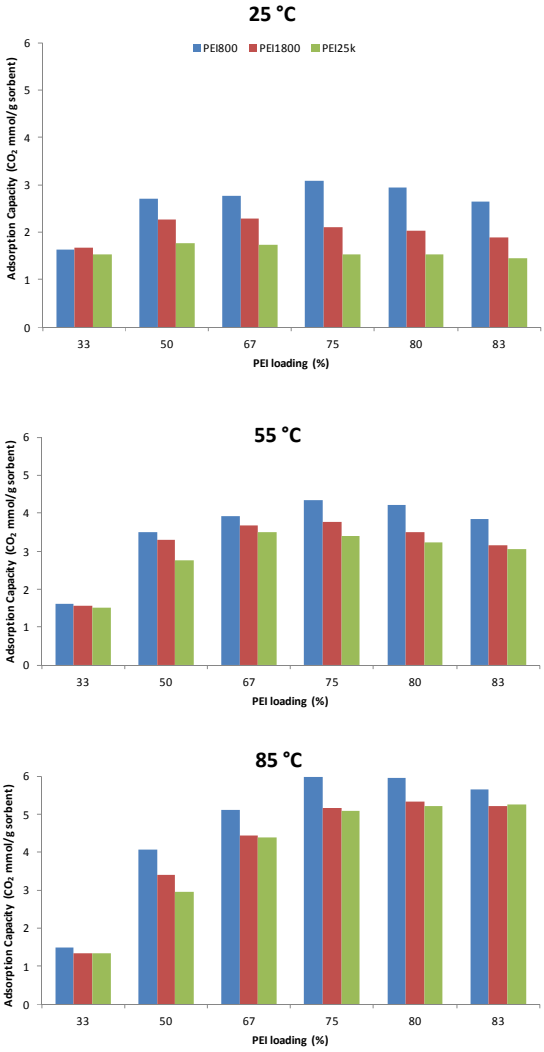

Fig. 12 Effect of the M_w of PEI on the adsorption capacity at various temperatures

Not unexpectedly, at 25 °C, the highest adsorption was observed for the adsorbent containing PEI with the lowest M_w (S5-PEI800), and decreased with increasing M_w of PEI regardless of the PEI concentration. The adsorption capacity for S5-PEI800 displayed a maximum at a PEI concentration of 75%. Above this concentration,

Table 8. CO_2 adsorption (mmol/g) on MCF/PEI25k containing various amounts of PEI25k at 25 °C, 55 °C and 85 °C

	50% PEI			67% PEI			75% PEI			80% PEI			83% PEI		
	25°C	55°C	85°C	25°C	55°C	85°C	25°C	55°C	85°C	25°C	55°C	85°C	25°C	55°C	85°C
S1	0.53	1.36	2.55	0.43	1.24	2.86									
S2	1.35	2.47	3.22	1.22	2.69	4.36	1.03	2.34	4.36						
S3	1.21	2.31	2.69	1.16	2.68	4.45	1.06	2.49	4.39	0.74	1.65	3.31			
S4	1.64	2.64	3.13	1.26	2.92	4.57	1.06	2.38	4.58	0.87	2.23	4.55			
S5	1.78	2.75	2.96	1.81	3.54	4.33	1.54	3.4	5.08	1.54	3.23	5.22	1.45	3.06	5.25

the addition of more PEI resulted in a decrease of the adsorption capacity, probably due to more PEI present in the pores of the support resulting in lower pore size and limiting the access of CO_2 to the active amino sites. On S5-PEI1800, the adsorption was similar with PEI concentrations between 50% and 75% and decreased at higher PEI contents. S5-PEI25k, prepared with the highest MW PEI, had the highest CO_2 adsorption capacity at a PEI concentration of 50%. Addition of more PEI had only a detrimental effect on the adsorption capacity at 25 °C The adsorbent containing only 33% PEI has in fact a higher adsorption capacity than the one containing 83% PEI25k.

With all three PEIs and all the PEI concentrations tested, the corresponding adsorbents adsorbed increasing amounts of CO_2 with increasing temperature, except for the adsorbents containing the lowest PEI concentration of 33%. At 55 °C and 85 °C, the CO_2 adsorption followed the same general pattern observed at 25 °C, i.e. a decrease in adsorption with increasing PEI M_w. However, the difference in adsorption capacity between the different PEI decreased with increasing temperature. At 85 °C, S5-PEI800 and S5-PEI1800 had almost similar adsorption capacity. With increasing temperatures, the highest adsorption capacity also shifted to higher PEI concentrations. This shift was most pronounced for S5-PEI25k which adsorbed the most at a PEI concentration of 80 to 83% at 85 °C compared to 50% at 25 °C. Chemically the three branched PEI used are very similar and differ mostly by their M_w. Therefore, the observed patterns seem to confirm the predominant role of physical properties, such as already mentioned viscosity, on the adsorption capabilities *(vide supra)*. At higher temperature, the viscosity of the PEI on the surface of the support diminishes allowing better access to the amino sites and diffusion of CO_2 and improving the reaction kinetics.[23, 33] A CO_2 adsorption of up to 6 mmol CO_2/g adsorbent was obtained with S5-PEI800-75 at 85 °C. The highest adsorption per g PEI was obtained with S5-PEI800-50 at 85 °C with 8.16 mmol CO_2/g PEI or 359 mg CO_2/g PEI (see SI, tables S2 and S3).

3.3.2 Stability of MCF-PEI adsorbents over numerous adsorption/desorption cycles. Besides being able to adsorb large amounts of CO_2, an effective adsorbent should also be easily regenerated and stable over numerous adsorption/desorption cycles. In order to test the chemical and thermal stability of our sorbents, they were submitted to a total of 100 short desorption/adsorption cycles (over 40 hours of cycling). Each cycle included a 10 min adsorption step under 95% CO_2 and a 15 min desorption step under nitrogen as a stripping gas. Both steps were run isothermally at 75 °C. For each cycle, the CO_2 adsorption capacity was determined by the difference in weight between the lowest point during each desorption and the highest point during the next adsorption phase. S5-PEIx-80 with x=800, 1800 and 25k were tested for their stability. The TGA plots for these measurements are presented in Figure 13. Figure 14 shows that regardless of the M_w of PEI, none of the sorbents underwent degradation within 100 cycles under these conditions. One reason could be that a large pore volume can accommodate more PEI inside the pores and be less affected by the formation of urea as proposed by Sayari et al.[53] In this work, we chose PEI with relatively high molecular weights. Although, PEIs with lower molecular weight, such as PEI 423 and TEPA, are generally reported to have higher adsorption capacity, they suffer from significant amine loss and therefore adsorption capacity loss as described in a number of previous multicycles studies.[42, 46, 47, 54-58]

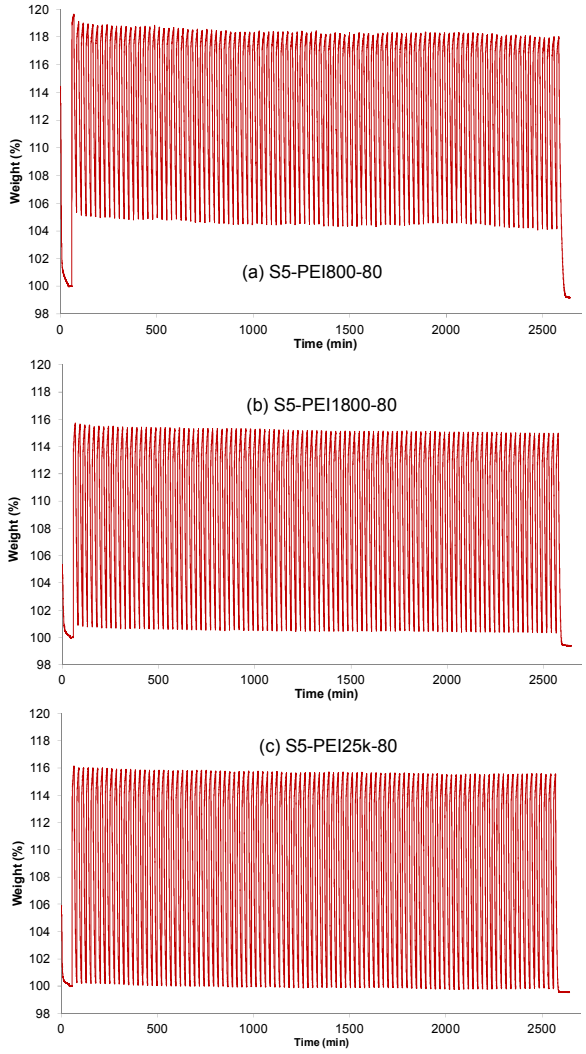

Fig. 13 TGA plot of 100 Adsorption/desorption cycles performed at 75 °C (10 min adsorption under CO_2, 15 min desorption under N_2) on (a) S5-PEI800-80, (b) S5-PEI1800-80, (c) S5-PEI25k-80.

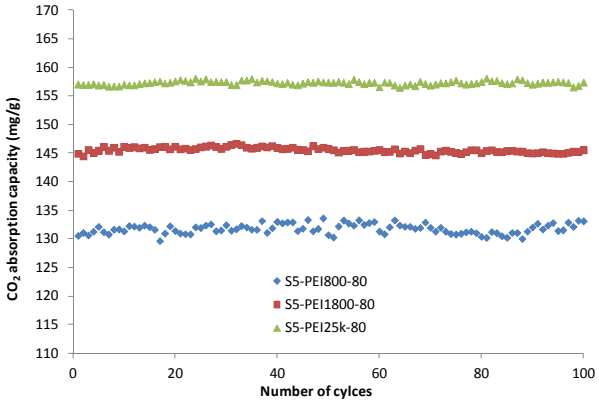

Fig. 14 Stability of S5-PEIx sorbents over 100 adsorption/desorption cycles at 75 °C (10 min adsorption under CO_2, 15 min desorption under N_2)

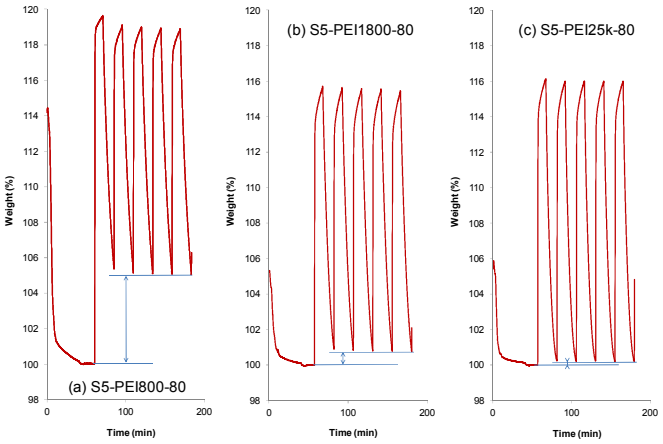

Fig. 15 First five adsorption/desorption cycles on S5-PEI-80 containing PEI with various M_w.

Interestingly in these short cycles, the adsorbent containing PEI with the highest M_w (25k) showed the largest cyclic CO_2 uptake (about 157 mg CO_2/g for S5-PEI25k-80), followed by S5-PEI1800-80 and S5-PEI800-80 (with the lowest M_w PEI). This had, however, more to do with the desorption step than the adsorption step as can be seen in Figure 15 showing the 5 first adsorption/desorption cycles of the three S5-PEI-80 tested. After desorption at 110 °C for 30 min the adsorbent with the lowest M_w PEI adsorbed the most CO_2 (almost 200 mg/g) during the first adsorption. The 15 min desorption at 75 °C were however insufficient and only 75% of the CO_2 could be desorbed, resulting in an apparent loss of adsorption capacity (Figure 16). The adsorbents prepared with PEI1800 and PEI25k had a lower initial adsorption capacity (close to 160 mg/g). Their desorption capacity was however higher with 95% for S5-PEI1800-80 and an essentially complete desorption for S5-PEI25k-80 (Figure 16a). Given enough time, all adsorbents were able to release all the CO_2 initially adsorbed. This indicates that adsorbents based on PEI with higher M_w have faster apparent desorption kinetics. This could be due to the fact that PEI with a higher M_w because of its size, does probably not penetrate as deep into the pores as lower molecular PEI and a larger part of the PEI remains outside the pores where access for CO_2 and its desorption are easier.

At lower PEI loadings this effect was less pronounced (Figure 16b-d) due to a better dispersion of the PEI on the surface of the support. However, even at a PEI concentration of 50%, the desorption on the adsorbent containing the PEI with the highest M_w was still the fastest (Figure 16d). On the other hand, the adsorption kinetics were very fast and similar regardless of the Mw of the PEI (Figure 17).

Overall, from these short adsorption/desorption cycle measurements it can be seen that up to a PEI concentration of 67%, the cyclic CO_2 adsorption capacity decreased with increasing PEI M_w, i.e. S5-PEI800 > S5-PEI1800 > S5-PEI25k (Figure 18). At a PEI concentration of 75%, however, the highest cyclic capacity was obtained with PEI1800 and at a PEI concentration of 80% with PEI25k. The overall highest cyclic adsorption capacity under these conditions was obtained with S5-PEI800-67 and S5-PEI-1800-75. Although the desorption kinetics were faster on PEI25k, it might therefore be more advantageous to use PEI with lower molecular weight to achieve high cycling capacity, but making sure that they do not suffer from leaching problems.

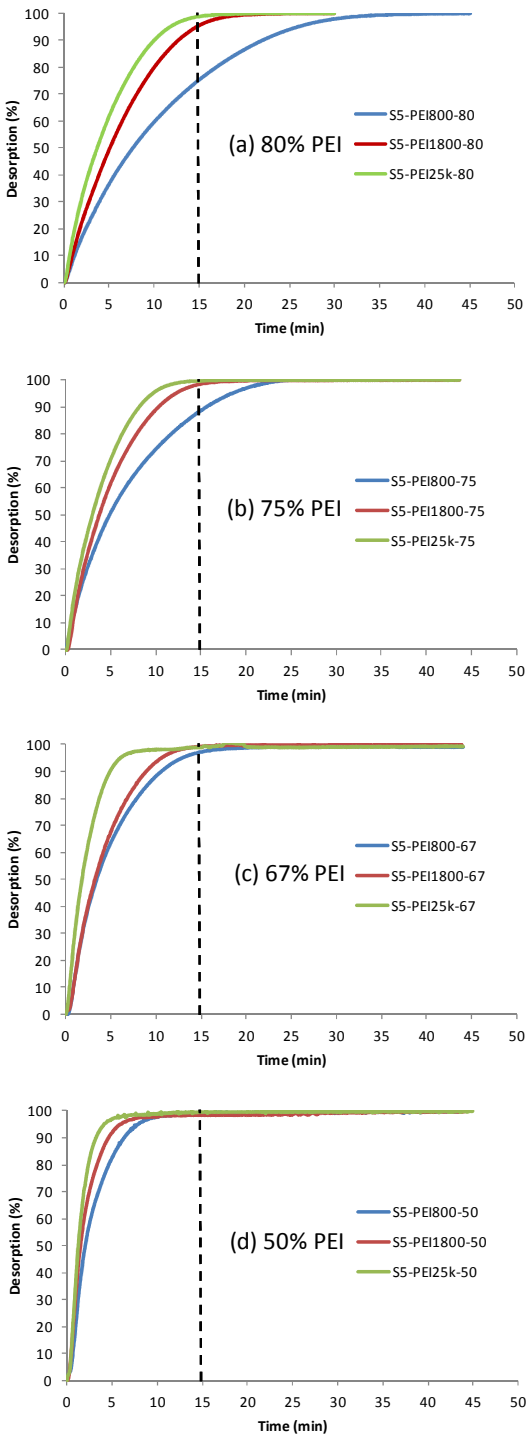

Fig. 16 Desorption capacity as a function of time for adsorbents containing PEI with various M_w and concentrations.

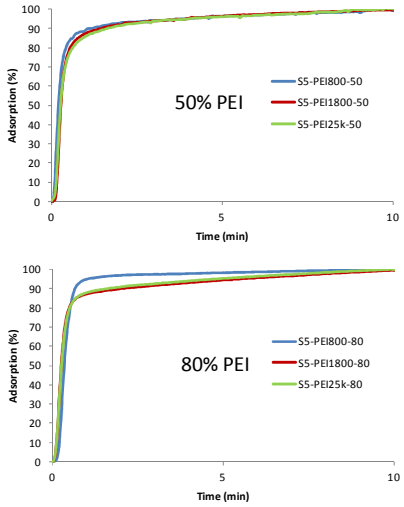

Fig. 17 Adsorption capacity as a function of time for the adsorbents containing PEI with various M_w and PEI concentrations of 50% and 80%.

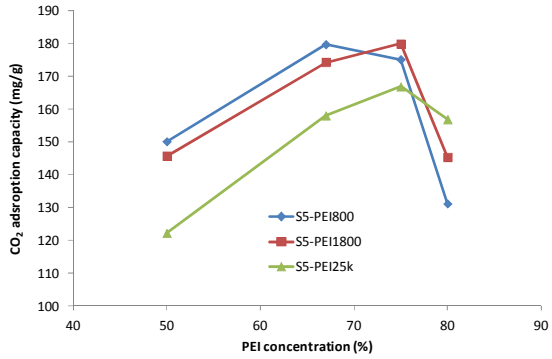

Fig. 18 Adsorption capacity in short adsorption/desorption cycles at 75 °C as a function of PEI M_w and concentration (average of 9 measurements, 10 min adsorption under CO_2, 15 min desorption under N_2, (see SI, Figure S4))

Conclusions

Mesocellular foams (MCF) with a broad range of pore volume and size were prepared by varying a number of synthesis parameters such as ammonium fluoride concentration, effect of swelling agent trimethylbenzene (TMB), equilibration time and calcination heating rates. The resulting materials featured pore volumes of up to 4.17 cm^3/g, significantly surpassing similar materials reported in the literature. Combined with a high surface area of 519 to 688 m^2/g, large pore diameter and interconnected wall structures, these materials were suitable for loading PEI. The obtained sorbents were tested for CO_2 adsorption capacity, kinetics, stability and regenerability.

When using PEI25k it was observed that the adsorption capacity at a given temperature and concentration of PEI increased with increasing pore volume and pore size of the support. This agrees with the suggestion that PEI loading and distribution on the support and consequently adsorption capacity benefits from larger pore size and/or larger pore volume. Adsorption up to 5.25 mmol CO_2/g adsorbent (230 mg/g) were obtained at 85 °C with the adsorbent based on the support with the highest pore volume. Decreasing PEI molecular weight resulted in increasing adsorption capacity. At 85 °C, the adsorbent based on PEI800 and the support with the highest pore volume resulted in CO_2 adsorption of up to 6 mmol/g (265 mg/g). At room temperature (25 °C) the highest adsorption was obtained with the adsorbent having a PEI concentration of 50%. However, as the temperature was increased to 55 °C followed by 85 °C, the maximum in adsorption shifted to adsorbents with higher PEI loadings.

The adsorption capacity of the adsorbents based on MCF and PEI did not decrease over 100 adsorption/desorption cycles at 75 °C. Interestingly, whereas the adsorption of CO_2 was similarly fast with all the PEIs, the desorption rate increased with increasing PEI molecular weight. PEI25k had the fastest desorption kinetics, regardless of PEI loading. Overall the highest adsorption capacity (about 180 mg/g, 4.1 mmol/g) using short adsorption/desorption cycles was obtained with S5-PEI800-67 and S5-PEI-1800-75.

The CO_2 adsorption results obtained here, especially at high PEI loadings, were in the top tier compared to the ones reported in the literature (see SI, table S4). Preparation of PEI based adsorbents clearly benefited from the utilization of support with larger pore volume which in turn led to improved CO_2 adsorption capabilities.

Acknowledgements

Support of our work by the Loker Hydrocarbon Research Institute and the United States Department of Energy is gratefully acknowledged.

Notes and references

[a] Loker Hydrocarbon Research Institute and Department of Chemistry, University of Southern California, University Park, Los Angeles, CA 90089-1661, United States.

Electronic Supplementary Information (ESI) available. See DOI: 10.1039/b000000x/

1 G. A. Olah, A. Goeppert and G. K. S. Prakash, *Beyond Oil and Gas: The Methanol Economy, 2nd ed.*, Wiley-VCH, 2009.
2 G. A. Olah, A. Goeppert and G. K. S. Prakash, *J. Org. Chem.*, 2009, **74**, 487.
3 G. A. Olah, G. K. S. Prakash and A. Goeppert, *J. Am. Chem. Soc.*, 2011, **133**, 12881-12898.
4 X. Xu and J. A. Moulijn, *Energy & Fuels*, 1996, **10**, 305-325.
5 C. Graves, S. D. Ebbesen, M. Mogensen and K. S. Lackner, *Renew. Sust. Energy Rev.*, 2011, **15**, 1-23.
6 A. Goeppert, M. Czaun, G. K. S. Prakash and G. A. Olah, *Energy Environ. Sci.*, 2012, **5**, 7833-7853.
7 A. Goeppert, M. Czaun, R. B. May, G. K. S. Prakash, G. A. Olah and S. R. Narayanan, *J. Am. Chem. Soc.*, 2011, **133**, 20164-20167.
8 C. W. Jones, *Annu. Rev. Chem. Biomol. Eng.*, 2011, **2**, 31-52.
9 N. MacDowell, N. Florin, A. Buchard, J. Hallett, A. Galindo, G. Jackson, C. S. Adjiman, C. K. Williams, N. Shah and P. Fennell, *Energy Environ. Sci*, 2010, **3**, 1645-1669.

10 *DOE/NETL Carbon Capture and Storage RD&D Roadmap*, National Energy Technology Laboratory, U.S. Department of Energy, 2010.
11 A. Kohl and R. Nielsen, *Gas Purification*, Gulf Publishing Company, Houston, Texas, 1997.
12 G. T. Rochelle, *Science*, 2009, **325**, 1652.
13 S. Choi, J. H. Drese and C. W. Jones, *ChemSusChem*, 2009, **2**, 796.
14 Q. Wang, J. Luo, Z. Zhong and A. Borgna, *Energy Environ. Sci*, 2011, **4**, 42-55.
15 D. M. D'alessandro, B. Smit and J. R. Long, *Angew. Chem. Int. Ed.*, 2010, **49**, 6058-6082.
16 E. J. Beckman, Pat. US 5 886 061, 1999.
17 M. Czaun, A. Goeppert, R. B. May, D. Peltier, H. Zhang, G. K. S. Prakash and G. A. Olah, *J. CO_2 Utilization*, 2013, **1**, 1-7.
18 G. Knowles, J. V. Graham, S. W. Delaney and A. L. Chaffee, *Fuel Process. Technol.*, 2005, **86**, 1435.
19 N. Hiyoshi, K. Yogo and T. Yashima, *J. Jpn. Pet. Inst.*, 2005, **48**, 29.
20 Y. Belmabkhout, R. Serna-Guerrero and A. Sayari, *Ind. Eng. Chem. Res.*, 2010, **49**, 359.
21 R. Serna-Guerrero, E. Da'na and A. Sayari, *Ind. Eng. Chem. Res.*, 2008, **47**, 9406.
22 P. J. E. Harlick and A. Sayari, *Ind. Eng. Chem. Res.*, 2007, **46**, 446.
23 A. Goeppert, S. Meth, G. K. S. Prakash and G. A. Olah, *Energy Environ. Sci.*, 2010, **3**, 1949-1960.
24 S. Meth, A. Goeppert, G. K. S. Prakash and G. A. Olah, *Energy & Fuels*, 2012, **26**, 3082-3090.
25 X. Xu, C. Song, J. M. Andresen, B. G. Miller and A. W. Scaroni, *Energy & Fuels*, 2002, **16**, 1463-1469.
26 X. Xu, C. Song, J. M. Andresen, B. G. Miller and A. W. Scaroni, *Micropor. Mesopor. Mat.*, 2003, **62**, 29-45.
27 T. Filburn, J. J. Helble and R. A. Weiss, *Ind. Eng. Chem. Res.*, 2005, **44**, 1542-1546.
28 A. Heydari-Gorji, Y. Belmabkhout and A. Sayari, *Langmuir*, 2011, **27**, 12411-12416.
29 A. D. Ebner, M. L. Gray, N. G. Chisholm, Q. T. Black, D. D. Mumford, M. A. Nicholson and J. A. Ritter, *Ind. Eng. Chem. Res.*, 2011, **50**, 5634-5641.
30 R. S. Franchi, P. J. E. Harlick and A. Sayari, *Ind. Eng. Chem. Res.*, 2005, **44**, 8007-8013.
31 H. A. Zinnen, R. Oroskar and C.-H. Chang, 4 810 266, 1989.
32 G. R. Stoneburner, 3 491 031, 1970.
33 X. Xu, C. Song, J. M. Andresen, B. G. Miller and A. W. Scaroni, *Energy and Fuels*, 2002, **16**, 1463.
34 X. Xu, C. Song, J. M. Andresen, B. G. Miller and A. W. Scaroni, *Microporous Mesoporous Mater.*, 2003, **62**, 29.
35 X. Xu, C. Song, B. G. Miller and A. W. Scaroni, *Fuel Process. Technol.*, 2005, **86**, 1457.
36 X. C. Xu, C. S. Song, B. G. Miller and A. W. Scaroni, *Ind. Eng. Chem. Res.*, 2005, **44**, 8113-8119.
37 V. Zeleňák, M. Badaničova, D. Halamová, J. Čejka, A. Zukal, N. Murafa and G. Goerigk, *Chem. Eng. J.*, 2008, **144**, 336-342.
38 W.-J. Son, J.-S. Choi and W.-S. Ahn, *Microporous Mesoporous Mater.* , 2008, **113**, 31-40.
39 X. Yan, L. Zhang, Y. Zhang, G. Yang and Z. Yan, *Ind. Eng. Chem. Res.*, 2011, **50**, 3220-3226.
40 P. Schmidt-Winkel, W. W. Lukens, P. Yang, D. I. Margolese, J. S. Lettow, J. Y. Ying and G. D. Stucky, *Chem. Mater.*, 2000, **12**, 686-696.
41 P. Schmidt-Winkel, W. W. J. Lukens, D. Zhao, P. Yang, B. F. Chmelka and G. D. Stucky, *J. Am. Chem. Soc.*, 1999, **121**, 254-255.
42 G. Qi, L. Fu, B. H. Choi and E. P. Giannelis, *Energy Environ. Sci.*, 2012, **5**, 7368-7375.
43 A. C. Voegtlin, F. Ruch, J. L. Guth, J. Patarin and L. Huve, *Microporous Mater.*, 1997, **9**, 95-105.
44 S. A. Bagshaw and I. J. Bruce, *Microporous Mesoporous Mater.*, 2008, **109**, 199-209.
45 N. Leventis, S. Mulik, X. Wang, A. Dass, V. U. Patil, C. Sotiriou-Leventis, H. Lu, G. Churu and A. Capecelatro, *J. Non-Crystalline Solids*, 2008, **354**, 632-644.
46 S.-H. Liu, W.-C. Hsiao and W.-H. Sie, *Adsorption*, 2012, **18**, 431-437.
47 W. Yan, J. Tang, Z. Bian and H. Liu, *Ind. Eng. Chem. Res.*, 2012, **51**, 3653-3662.
48 J. Zhao, F. Simeon, Y. Wang, G. Luo and A. Hatton, *RSC Adv.*, 2012, **2**, 6509-6519.
49 D. J. N. Subagyono, Z. Liang, G. Knowles and A. L. Chaffee, *Chem. Eng. Res. Design*, 2011, **89**, 1647-1657.
50 W. Chaikittisilp, R. Khunsupat, T. T. Chen and C. W. Jones, *Ind. Eng. Chem. Res.*, 2011, **50**, 14203-14210.
51 W. Li, P. Bollini, S. Didas, S. Choi, J. H. Drese and C. W. Jones, *ACS Appl. Mater. Interfaces*, 2010, **2**, 3363-3372.
52 Z. Liang, B. Fadhel, C. J. Schneider and A. L. Chaffee, *Adsorption*, 2009, **15**, 429-437.
53 A. Sayari and Y. Belmabkhout, *J. Am. Chem. Soc.*, 2010, **132**, 6312-6314.
54 C. Chen, S.-T. Yang, W.-S. Ahn and R. Ryoo, *Chem. Commun.*, 2009, 3627-3629.
55 Y. Liu, J. Shi, J. Chen, Q. Ye, H. Pan, Z. Shao and Y. Shi, *Micropor. Mesopor. Mat.*, 2010, **134**, 16-21.
56 X. Wang, H. Li, H. Liu and X. Hou, *Micropor. Mesopor. Mat.*, 2011, **142**, 564-569.
57 W. Wang, X. Wang, C. Song, X. Wei, J. Ding and J. Xiao, *Energy & Fuels*, 2013, **27**, 1538-1546.
58 G. G. Qi, Y. B. Wang, L. Estevez, X. N. Duan, N. Anako, A. H. A. Park, W. Li, C. W. Jones and E. P. Giannelis, *Energy Environ. Sci.*, 2011, **4**, 444-452.

